

# Near-Infrared Spectroscopic Measurement of Urea in Dialysate Samples Collected During Hemodialysis Treatments

CHRISTOPHER V. EDDY, MICHAEL FLANIGAN, and MARK A. ARNOLD\*

Department of Chemistry, Optical Science and Technology Center (C.V.E., M.A.A.), and Department of Internal Medicine (M.F.), University of Iowa, Iowa City, Iowa 52242

Single-beam spectra were collected over the combination region of the near-infrared spectrum for 80 samples collected from 15 people over a two-week period. Partial least-squares (PLS) regression was used to generate an optimized calibration model for urea. PLS calibration models accurately measure urea in the spent dialysate matrix. Prediction errors are on the order of 0.15 mM, which is sufficient for the clinical assessment of the dialysis process. In addition, the feasibility of a global calibration model is demonstrated by generating a calibration model from samples and spectra obtained from 12 people to predict the level of urea in samples collected from 3 different people. In this case, the standard error of prediction is 0.09 mM. Spectra were modified in order to systematically examine the impact of resolution and noise. Little impact is observed by altering the spectral resolution from 4 to 32  $\text{cm}^{-1}$ . Spectral noise, however, plays an important role in the accuracy of these calibration models. Increasing the magnitude of the spectral noise increases the prediction errors and increases the width of the spectral range necessary for extracting the analytical information. The utility of the method is demonstrated by analyzing dialysate samples collected during actual dialysis treatments. In addition, the necessary resolution and spectral quality necessary for reliable *on-line* urea monitoring is identified. These findings indicate that a dedicated, *on-line* urea spectrometer must possess a resolution of 16  $\text{cm}^{-1}$  coupled with a sample thickness of 1.5 mm and spectral noise levels on the order of 25 micro-absorbance units when measured as the root-mean-square (RMS) noise of 100% lines.

Index Headings: Near-infrared spectroscopy; Hemodialysis; Urea; Partial least-squares regression; PLS; Noninvasive chemical sensing.

## INTRODUCTION

A continuous monitor to chemically follow the hemodialysis process is critical for enhancing the effectiveness of this life-saving treatment. While no single molecule accounts for all the toxicity of kidney failure, urea is the solute of choice for quantifying dialysis therapy. The principal metric for quantifying dialysis therapy is the dialysis dose, which is determined as  $Kt/V$ , where  $K$  is the dialyzer clearance,  $t$  is the duration of dialysis, and  $V$  is the total blood volume within which the urea is distributed. For each treatment, the targeted dialysis dose is 1.3 or greater. During the last two decades both urea clearance and the time-averaged concentration of urea in the patient's plasma have been correlated with patient outcomes.<sup>1,2</sup> Current estimates are that each 0.1 unit change in the dialysis dose results in a 7% change in the patient's annual mortality risk.<sup>3</sup>

Unfortunately, dialysis dosage is not monitored during routine treatment. In fact, the actual dialysis dose is documented in fewer than 10% of all dialysis treatments and 25% of these monitored treatments do not meet the minimum criteria ( $Kt/V \geq 1.3$ ) for adequate therapy.<sup>4</sup> Furthermore, it is likely that only 25% of all dialysis sessions provide therapy equal to or greater than the 10% of dialysis treatments that are monitored. Research indicates that dialysis treatments in general are under performed,<sup>5</sup> which adversely affects mortality of people with end-stage renal disease.

Attempts to monitor the hemodialysis process center on the measurement of urea collected in the spent dialysate. Several urea biosensors have been proposed for this purpose.<sup>6-9</sup> In these devices, urease enzymatically converts the collected urea to ammonium and bicarbonate ions and these ions are detected electrochemically. Implementation of this biosensor technology is slow because of the added costs associated with the required reagents.

We are interested in exploring the utility of near-infrared spectroscopy for directly measuring urea in spent dialysate. In this method, incident near-infrared light passes through a sample of the dialysate fluid, and the concentration of urea is determined from an analysis of the resulting spectrum. No chemical reagents are needed for this measurement, which can potentially reduce the cost of analysis compared to the above-mentioned biosensor approach. The ability to measure urea in the dialysate fluid matrix has been demonstrated.<sup>10</sup> In this initial report, the combination region of the near-infrared spectrum (5000–4000  $\text{cm}^{-1}$ ) was identified as the best spectral range for measuring urea. In addition, standard dialysate solutions composed of known concentrations of urea and glucose were used to establish the limit of detection of this approach. Standard errors of prediction for urea were on the order of 0.3 to 0.4 mM. Finally, the ability to measure urea in spent dialysate samples was demonstrated from an analysis of spectra obtained from five samples, which were collected during actual dialysis treatments.

Our development of near-infrared spectroscopy for hemodialysis monitoring is continued in this paper by expanding our analysis of actual dialysate samples to eighty samples collected over a six-day period from fifteen individuals. In addition, critical measurement parameters are evaluated. Calibration models are generated from single-beam spectra and the impact of replicate measurements is evaluated. Also, the effects of spectral resolution

Received 15 January 2003; accepted 27 May 2003.

\* Author to whom correspondence should be sent. E-mail: mark-arnold@uiowa.edu.

and spectral noise are characterized in a systematic manner. Each of these three parameters is important for the development of a dedicated spectrometer unit for measuring urea continuously during the dialysis process.

## EXPERIMENTAL

**Instrumentation.** Spectra were collected with a Nicolet Magna 550 Fourier transform spectrometer (ThermoNicolet, Madison, WI). This spectrometer was equipped with a standard 20-watt tungsten halogen lamp, calcium fluoride beam splitter, and cryogenically cooled indium antimonide (InSb) detector. An interference filter (Barr and Associates, Inc.) was placed in the optical path before the sample to restrict the spectrum to 5000–4000  $\text{cm}^{-1}$ . Samples were held in a Wilmad sample holder equipped with 25-mm-diameter sapphire windows. Teflon spacers were used to maintain a 1.5 mm sample thickness. This solution thickness represents an attempt to increase the magnitude of absorbance and is nearly ideal for the combination of source and detector, as treated recently by Jensen and Bak.<sup>11</sup> Solution temperature was held at  $37.0 \pm 0.1$  °C by circulating thermostated water from a VWR model 1140 water bath. Each sample was allowed to thermally equilibrate in the sample cell before the first spectrum was collected. Generally, a five-minute equilibration period was used for this purpose.

**Materials.** All chemical reagents were purchased from Sigma Chemical Co. (St. Louis, MO). Sodium hypochlorate was purchased as an aqueous solution with 4% available chlorine. Type III Jack Bean urease was purchased with a specific activity of 31 000 units per gram. All solutions were prepared with distilled-deionized reagent grade water that was obtained from a Milli-Q water purification unit.

**Sample Collection.** Hemodialysis samples were collected directly from the dialyzer during typical dialysis treatments at the University of Iowa Hospitals and Clinics. Samples were collected from fifteen unique subjects on six different days over the span of two weeks. For each sample, 15 mL of spent dialysate solution was collected and stored at room temperature for approximately three hours before being transported to our research laboratory for analysis. The concentration of urea in each sample was determined on the day it was collected. The urease/Berthelot reaction scheme was used to provide these reference urea concentrations. Details of this method are described elsewhere.<sup>12</sup> Near-infrared spectra were also collected the same day the sample was obtained. In total, eighty spent dialysis samples were obtained for analysis.

**Data Analysis.** Near-infrared spectra were collected in triplicate for each sample. Replicate spectra were collected sequentially without removing the sample from the instrument. Spectra were collected as 256 coadded interferograms. The resulting interferogram was triangularly apodized and Fourier processed with the software resident within the Omnic operating system (version 5b) used to operate the spectrometer. This process produced single-beam spectra with a 2  $\text{cm}^{-1}$  point spacing and 4  $\text{cm}^{-1}$  resolution. Subsequent spectral processing was accomplished on an Iris Indigo computer (Silicon Graphics, Inc.). All processing was performed with software tools

provided by Professor Gary W. Small, from the Center for Intelligent Chemical Instrumentation in the Department of Chemistry and Biochemistry at Ohio University, Athens, OH. In all cases, calibration models were generated from single-beam spectra with no mean centering, no normalization, and no windowing.

Partial least squares (PLS) regression<sup>13,14</sup> was used to generate calibration models. Optimum conditions of spectral region and number of factors were established as detailed elsewhere.<sup>15,16</sup> Briefly, the full set of data was split into calibration and prediction subsets. The prediction data consisted of all spectra associated with 13 randomly selected samples (39 spectra). Unless indicated otherwise, samples for the predict set were selected randomly, except that care was taken to exclude samples with the highest and lowest urea concentrations from the prediction data. Spectra in the prediction data set were not used to generate the calibration model, but to test the accuracy of such models. The remaining calibration data were split three times into training and monitoring subsets as described before.<sup>15,16</sup> These training and monitoring data were used to establish optimal conditions of number of PLS factors and spectral range. The final calibration models were generated by applying the optimized parameters to the full set of calibration data. Model performance was characterized by the standard error of calibration (SEC), standard error of prediction (SEP), and mean percent error (MPE), as defined elsewhere.<sup>16</sup>

Spectral resolution was varied by reprocessing modified interferograms. The collected interferograms produced single-beam spectra with 2  $\text{cm}^{-1}$  point spacing or 4  $\text{cm}^{-1}$  spectral resolution. Interferograms were collected as 16-k, double-sided interferograms with no zero-filling. Each interferogram was reduced in size to a series of single-beam spectra with lower resolution. As a result, 8-k interferograms produced spectra with 4  $\text{cm}^{-1}$  point spacing and 8  $\text{cm}^{-1}$  resolution, 4-k interferograms produced spectra with 8  $\text{cm}^{-1}$  point spacing and 16  $\text{cm}^{-1}$  resolution, and 2-k interferograms produced spectra with 16  $\text{cm}^{-1}$  point spacing and 32  $\text{cm}^{-1}$  resolution. In all cases, no zero-filling was used. These calculations were performed by using an option in the Omnic operating system.

Spectral noise was modified by adding Gaussian distributed random noise to individual single-beam spectra. The collected single-beam spectra, which were obtained from 16-k interferograms, had a composite noise level of approximately 2 micro-absorbance units ( $\mu\text{AU}$ ). This noise level corresponds to the root-mean-square (RMS) noise over the 4500–4400  $\text{cm}^{-1}$  region of 100% lines. Noise levels on 100% lines were obtained by dividing replicate spectra for the same sample, converting to absorbance units, fitting the resulting data to a second-order polynomial function, and then computing the RMS between each data point and the fitted function. By fitting the 100% line to a second-order polynomial, one is able to eliminate the impact of temperature variance on the RMS noise calculation, thereby giving a better indication of the instrumental signal-to-noise ratio. Details of this procedure are provided elsewhere.<sup>17</sup> Spectral noise was added to single-beam spectra to generate four unique sets of spectra with average RMS noise values of approximately 15, 30, 60, and 120  $\mu\text{AU}$ . For each single-beam

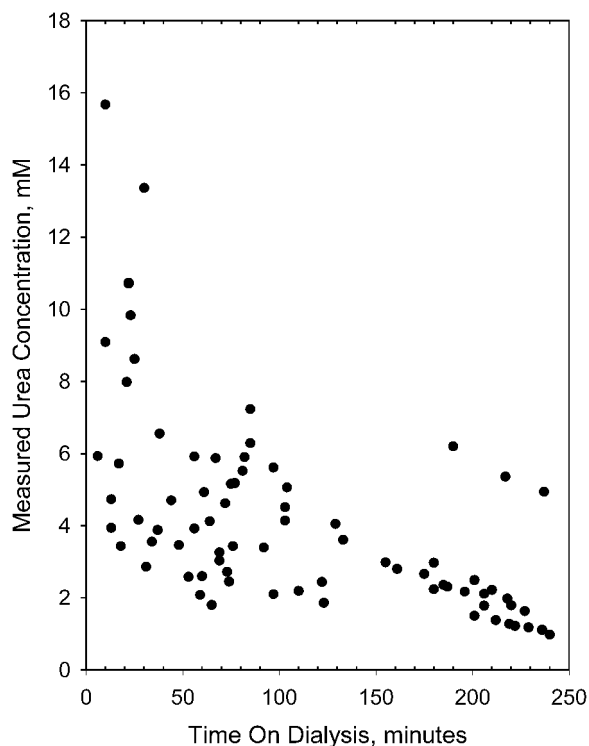


Fig. 1. Distribution of urea concentrations in collected samples as a function of elapsed time of dialysis treatment.

spectrum, a unique Gaussian distributed noise spectrum was generated, then scaled to the desired magnitude, and finally added to the spectrum.

## RESULTS AND DISCUSSION

During the course of a hemodialysis treatment, the concentration of urea decreases in the spent dialysate as the pool of systemic blood equilibrates with the pool of dialyzed blood. This systematic reduction in urea concentration is evident in the urea concentrations in samples used in this work. Figure 1 illustrates the dependency of the urea concentration on elapse time of dialysis treatment. These data show a general trend toward lower urea concentrations over the course of the treatment. A smooth curve is not observed because these data correspond to a composite of 15 unique patients with sampling for each patient occurring over separate dialysis treatments. For this entire data set, the mean urea concentration is 4.22 mM, the standard deviation is 2.89 mM, the median concentration is 3.43 mM, and the range extends from 0.98 to 15.7 mM.

Temporal correlations within a data set can potentially result in apparently functioning calibration models, which are based on systematic co-variance between the analyte concentration and instrument signal.<sup>18</sup> Undesirable situations like this can be avoided by minimizing correlations between time and analyte concentration. In this work, such correlations were minimized by collecting only a few samples from each subject during a particular dialysis treatment. In addition, the probability of correlations between urea concentration and instrument signal was further reduced by collecting and analyzing samples on arbitrarily selected days over a two-week period.

TABLE I. Mean RMS noise levels of 100% lines computed from first and second spectra collected for all eighty dialysate samples.

Spectral range, $\text{cm}^{-1}$	RMS noise, $\mu\text{AU}$	Spectral range, $\text{cm}^{-1}$	RMS noise, $\mu\text{AU}$
5000–4900	3460	4500–4400	2.26
4900–4800	115	4400–4300	6.05
4800–4700	10.2	4300–4200	54.0
4700–4600	2.91	4200–4100	1720
4600–4500	1.89	4100–4000	10 000

**Calibration Models.** Initial urea calibration models were generated with all 240 spectra from 80 samples and with randomly selecting samples for the prediction data set. All spectra associated with 13 randomly selected samples (39 spectra) were placed in the prediction data set, while all spectra for the remaining 67 samples (201 spectra) were used for calibration purposes. The quality of these spectra was determined by computing the RMS noise on 100% lines across the full set of 80 samples. In this calculation, the RMS noise was measured for the first and second single-beam spectra for each sample. Table I summarizes the average RMS noise across all samples for every  $100 \text{ cm}^{-1}$  segment of the spectrum. Large noise levels at the extremes correspond to low light levels at the detector, which is caused by the extensive attenuation of the incident light by the strong absorption properties of water.<sup>19</sup> Noise levels range from 1.89 to  $54.0 \mu\text{AU}$  between  $4800$  and  $4200 \text{ cm}^{-1}$ .

The optimum calibration model for urea in spent dialysate samples requires five PLS factors and a spectral range of  $4770\text{--}4450 \text{ cm}^{-1}$ . This spectral range encompasses the two main absorption features of urea in this spectral region.<sup>10</sup> These bands are centered at  $4650$  and  $4550 \text{ cm}^{-1}$  and correspond to combinations of symmetric and asymmetric vibrational N–H stretches coupled with the N–H bending vibrations.<sup>10,20</sup> A standard *F*-test was used to verify, at the 95% confidence level, the statistical merit of these five factors. The SEC and SEP are 0.13 and 0.14 mM, respectively, and the MPE is 2.5% for this calibration model. Results for this model are presented in Fig. 2 as a concentration correlation plot. In this plot, the concentration of urea predicted from the calibration model is plotted as a function of the concentration of urea determined from the reference method. Data points from both the calibration and prediction data sets fall along the ideal unity correlation, which is presented as the solid line. The corresponding residual plot is provided in the inset. No systematic variance is noted in the residuals as a function of urea concentration.

The above-described calibration model was developed on the basis of a random splitting of the complete data set. Although all spectra for each sample were moved together into calibration and prediction data sets, this is not true for spectra collected from each subject. This random splitting procedure does not separate spectra by individual, so spectra from individual subjects are likely in both the prediction and calibration data sets. A more rigorous calibration model can be developed by splitting the calibration and prediction data sets according to all spectra associated with individual subjects. Such a splitting strategy simulates a global calibration model where urea concentrations can be determined for subjects not repre-

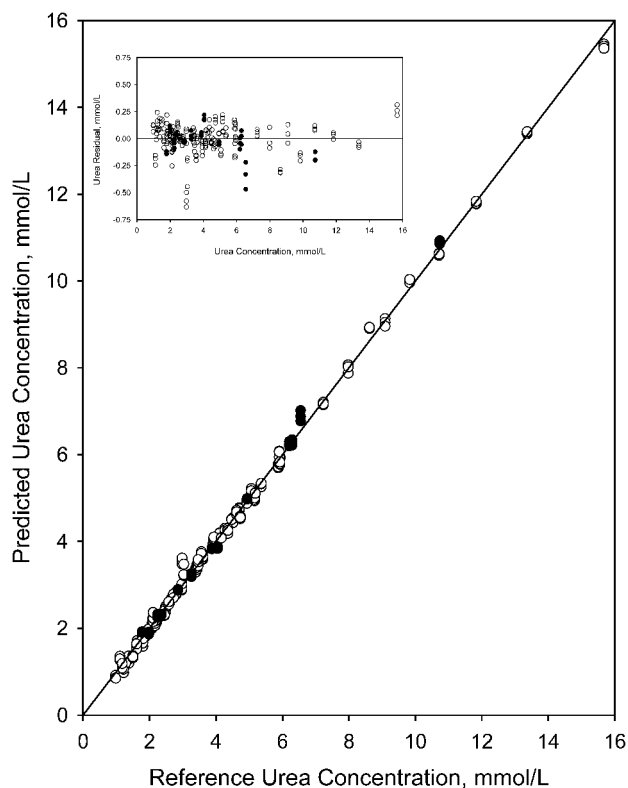


Fig. 2. Concentration correlation plot for PLS calibration model based on random splitting of urea samples and the corresponding triplicate spectra, showing calibration data (open circles), prediction data (closed circles), and ideal unity correlation (solid line). Inset shows urea residuals as a function of urea concentration for the calibration data (open circles) and prediction data (closed circles).

sented in the calibration data set. Clearly, a global calibration model would be more clinically useful than one requiring individual calibration for each subject.

To demonstrate the potential of a global calibration model, all spectra generated from three subjects were selected as the prediction data set and the spectra from the remaining twelve subjects were assigned to the calibration data set. The three prediction subjects were selected arbitrarily and resulted in 14 unique samples and 42 spectra. The optimized calibration model for this splitting of the data requires five PLS factors and a spectral range of 4770–4500  $\text{cm}^{-1}$ . SEC and SEP values are 0.20 and 0.10 mM, respectively, and the MPE is 1.5%. These results are essentially identical to those obtained for the random splitting of the data, which supports the possibility of a global calibration. There are certainly small differences in the chemical composition of samples collected across subjects, but these chemical differences do not interfere with the PLS calibration model for urea.

In a clinical setting, the collection of triplicate spectra may be impractical because of the added time and expense. In addition, continuous monitoring during dialysis treatments demands rapid data acquisition in order to minimize urea concentration changes during the measurement. To address these issues, a calibration model was developed using only one spectrum per sample to determine the advantage, if any, of processing triplicate spectra over a single spectrum.

The calibration and prediction data sets used in this

TABLE II. Impact of spectral resolution on PLS models and model performance.

Resolution, $\text{cm}^{-1}$	Spectral range, $\text{cm}^{-1}$	Number of PLS factors	SEC, mM	SEP, mM	MPE, %
4	4780–4470	5	0.13	0.09	2.1
8	4600–4450	5	0.15	0.12	2.8
16	4600–4500	4	0.17	0.14	4.0
32	4610–4430	5	0.18	0.11	2.6

experiment are the same as those detailed above where samples are split randomly. In this case, however, only the first spectrum of the triplicate is used in the data processing. The resulting calibration model uses five PLS factors and a spectral range of 4770–4500  $\text{cm}^{-1}$ . The SEC and SEP are 0.13 and 0.09 mM, respectively, and the MPE is 2.1%. This calibration performance is similar to the model based on all replicate spectra. Additional experiments indicated that similar results are obtained regardless of the spectrum taken from the group of triplicates for each sample. This last finding indicates little difference between replicate spectra, which is consistent with the low spectral noises reported above for the corresponding 100% lines.

**Spectral Resolution.** The calibration models detailed above were prepared from spectra collected with a research grade Fourier transform infrared (FT-IR) spectrometer operating at 4  $\text{cm}^{-1}$  resolution. The impact of spectral resolution was investigated by reprocessing these spectra with lower resolution and repeating the model optimization procedure. The original 4  $\text{cm}^{-1}$  resolution data were reprocessed to produce spectra with resolutions of 8, 16, and 32  $\text{cm}^{-1}$ . Optimized calibration models were established independently for each resolution setting. In these models, only one spectrum was used for each sample. The principal findings are summarized in Table II.

No major differences in model performance are evident from the results listed in Table II. Each calibration model required 4 or 5 factors, and values for the SEC, SEP, and MPE are similar for each spectral resolution. The optimized spectral range shifts from 4770–4600  $\text{cm}^{-1}$  for the 4  $\text{cm}^{-1}$  resolution model to 4610–4430  $\text{cm}^{-1}$  for the 32  $\text{cm}^{-1}$  resolution model. Magnitude of the spectral range remains relatively constant across these resolutions, with ranges of 170, 150, 100, and 180  $\text{cm}^{-1}$  for 4, 8, 16, and 32  $\text{cm}^{-1}$  resolutions, respectively. The number of resolution elements used in these calibration models decreases as the resolution decreases. Specifically, 85, 38, 13, and 11 resolution elements are used, respectively, for models based on 4, 8, 16, and 32  $\text{cm}^{-1}$  resolution spectra.

The above treatment of resolution does not take into consideration the impact of analysis time. In the above experiment, lower resolution spectra are generated simply by truncating and reprocessing the 4  $\text{cm}^{-1}$  resolution interferograms. It is well known, however, that less time is required to collect lower resolution spectra under conditions of identical mirror velocities.<sup>21</sup> For a fixed analysis time, more low resolution spectra can be collected and signal averaged, thereby providing lower noise and superior model performance. The additional number of spectra obtainable during this difference in time depends

**TABLE III. PLS calibration models for urea with different spectral quality for each spectral resolution.**

Resolution	RMS noise, $\mu\text{AU}$	Spectral range, $\text{cm}^{-1}$	Number of PLS factors	SEC, mM	SEP, mM	MPE, %
4	2.3	4780–4470	5	0.13	0.09	2.1
4	14	4740–4500	5	0.21	0.11	2.6
4	26	4750–4450	5	0.25	0.15	3.9
4	52	4590–4200	5	0.45	0.52	13.3
4	103	4640–4170	5	0.54	0.62	17.0
8	1.5	4600–4450	5	0.15	0.12	2.8
8	14	4790–4450	5	0.19	0.13	3.2
8	28	4700–4500	5	0.26	0.30	9.2
8	57	4880–4400	5	0.38	0.27	7.0
8	110	4820–4370	5	0.54	0.45	14.0
16	1.1	4600–4500	4	0.17	0.14	4.0
16	16	4840–4440	5	0.22	0.24	6.5
16	31	4900–4350	6	0.36	0.23	6.4
16	63	4800–4390	5	0.49	0.33	10.4
16	130	4800–4370	4	0.74	0.68	22
32	1.0	4610–4430	5	0.18	0.11	2.6
32	17	4890–4410	5	0.34	0.36	9.2
32	33	4780–4190	5	0.52	0.45	15.2
32	66	4810–4350	4	0.68	0.63	21
32	130	4800–4100	5	1.09	0.96	32

greatly on the duty-cycle of the moving mirror within the interferometer and, therefore, cannot be determined in general. Nevertheless, under detector-noise-limited conditions and using a fixed data collection period, lower resolution spectra will be less noisy and, therefore, preferred.

**Spectral Noise.** The original  $4\text{ cm}^{-1}$  resolution spectra were collected with a cryogenically cooled indium antimonide detector, which provided RMS noise levels of approximately  $2\ \mu\text{AU}$ . The spectral noise was systematically increased in these data to estimate the impact of reducing spectral quality on the predictive ability of the calibration model. Sixteen data sets were generated by adding four levels of noise to each of the four resolution levels. In total, twenty calibration models were constructed, corresponding to five noise levels (the endogenous noise level of the original data plus the four added noise levels) coupled with four resolution levels. Again, a single spectrum was taken for each sample. The calibration and prediction data sets consisted of 67 and 13 spectra, respectively, and the same splitting of these spectra was used to construct each calibration model. Results are tabulated in Table III.

Several interesting trends are evident from the values in Table III. First, increasing the RMS noise degrades the prediction accuracy of the models. Both the SEC and SEP increase with increasing noise or decreasing spectral quality. The relationship between the prediction error and the RMS noise of 100% lines is demonstrated in the plot shown in Fig. 3. Data for each resolution setting are fitted individually to a linear function. In all cases, a linear model fits the points with slopes of 0.0047, 0.0033, 0.0042, and 0.0064  $\text{mM}/\mu\text{AU}$  for resolutions of 4, 8, 16, and  $32\text{ cm}^{-1}$ , respectively. The slope term for these linear fits provides a measure of the sensitivity of the prediction error to spectral quality. These slopes indicate that a 0.25 mM increase in the prediction error requires an approximately 50  $\mu\text{AU}$  increase in the RMS noise. In this case,

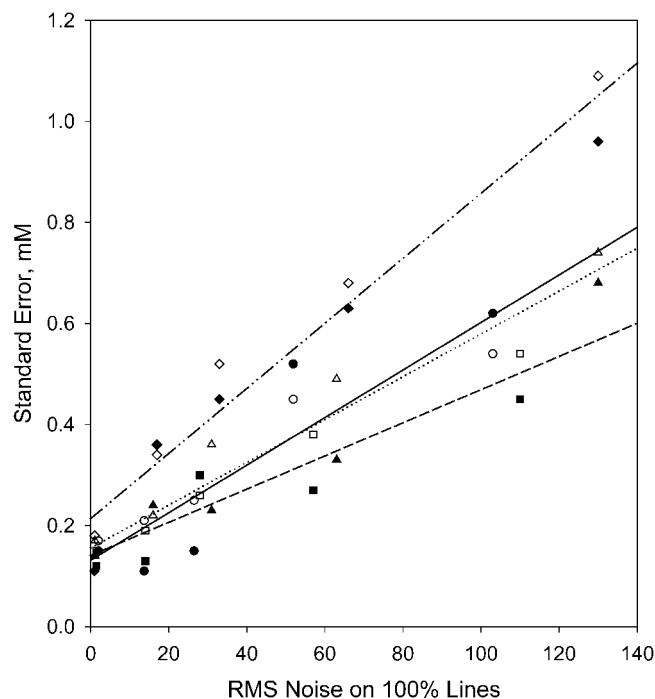


**FIG. 3.** Relationship between measurement accuracy and spectral quality where standard error of calibration (open symbols) and standard error of prediction (closed symbols) are plotted as functions of RMS noise levels of 100% lines over the  $4600\text{--}4500\text{ cm}^{-1}$  spectral range for spectra with resolutions of  $4\text{ cm}^{-1}$  (circles, solid line),  $8\text{ cm}^{-1}$  (triangles, dashed line),  $16\text{ cm}^{-1}$  (squares, dotted line), and  $32\text{ cm}^{-1}$  (diamonds, dashed-dot line). Lines correspond to linear least-squares fits to the corresponding data.

prediction errors are not overly sensitive to spectral quality as measured by the RMS noise of 100% lines.

The y-intercept terms for the fitted points in Fig. 3 provide an estimate of the minimum standard error possible, or the error when the RMS noise is zero. The y-intercept values from Fig. 3 are 0.13, 0.14, 0.16, and 0.21 mM for the 4, 8, 16, and  $32\text{ cm}^{-1}$  resolutions, respectively. The average of these values is 0.16 mM, which is a reasonable estimate of the uncertainty in the reference urea concentrations taken from the urease/Berthelot method.

As the noise increases, the amount of spectral information required for optimum model performance increases. This trend corresponds to a widening of the spectral range for higher noise levels. In general, this trend is observed within each of the tested resolution settings. The widest spectral range corresponds to the  $32\text{ cm}^{-1}$  resolution spectra with  $130\ \mu\text{AU}$  RMS noise. In this case, the spectral range is  $4800\text{--}4100\text{ cm}^{-1}$ , which corresponds to essentially all of the available spectral information. Combination spectra collected from aqueous solutions are typically limited to the  $4800\text{--}4200\text{ cm}^{-1}$  spectral range because of the strong absorbance properties of water.<sup>19</sup> Although wider spectral ranges are needed for noisier spectra, the number of PLS factors necessary to model the system remains relatively constant. Five factors are required in the majority of models.

## CONCLUSION

The results presented here demonstrate the feasibility of measuring urea noninvasively in spent dialysate sam-

ples. Samples collected during actual dialysis treatments can be analyzed for urea with a standard error of prediction of 0.15 mM. Such calibration models are possible from near-infrared spectra collected over the combination region of the near-infrared spectrum (5000–4000  $\text{cm}^{-1}$  or 2.0–2.5  $\mu\text{m}$ ). Furthermore, these results suggest that a global calibration is possible. The ability to accurately predict urea concentration for subjects not represented in the calibration data set demonstrates the selectivity offered by this approach. Finally, sufficient analytical information is available in a single spectrum, which eliminates the need to collect replicate spectra for each sample. The ability to measure urea from a single spectrum reduces the time of analysis, which may be an important feature for a future *on-line* device to continuously measure urea during the dialysis process.

Spectral resolution and spectral quality were evaluated to determine the impact of these parameters on the ability to measure urea. These parameters represent the principal instrumental specifications that must be considered to develop a dedicated spectrometer system for measuring urea *on-line*. As determined from truncated interferograms, model performance is independent of spectral resolution over a range of 4 to 32  $\text{cm}^{-1}$ . Spectral quality, on the other hand, impacts model performance with an increase in the magnitude of prediction errors as a function of higher spectral noise, as determined by the RMS noise of 100% lines. In practice, lower resolution spectra permit greater signal averaging over a set time period, thereby providing higher quality spectra and superior calibration models.

For PLS calibration models, the limit of detection can be estimated as three times the standard error of calibration and prediction. Considering a targeted limit of detection of 1 mM for dialysis monitoring, an *on-line* urea spectrometer must provide a standard error of 0.33 mM. According to the data listed in Table III, such models can be obtained with several combinations of resolution and spectral quality. This level of performance is achieved with the following pairs of resolution and RMS noise of 100% lines: 4  $\text{cm}^{-1}$  and 26  $\mu\text{AU}$ ; 8  $\text{cm}^{-1}$  and 28  $\mu\text{AU}$ ; 16  $\text{cm}^{-1}$  and 31  $\mu\text{AU}$ ; and 32  $\text{cm}^{-1}$  and 17  $\mu\text{AU}$ . These data suggest that sufficient model accuracy is possible

from a dedicated spectrometer capable of providing combination spectra with 16  $\text{cm}^{-1}$  resolution and RMS noise levels on the order of 25  $\mu\text{AU}$ .

#### ACKNOWLEDGMENT

This work was sponsored by a grant from the National Institutes of Diabetes and Digestive and Kidney Diseases (DK-45126).

1. E. G. Lowrie, N. M. Laird, T. A. Parker, and J. A. Sargent, *New Engl. J. Med.* **305**, 1176 (1981).
2. W. F. Owen, N. L. Lew, Y. Liu, E. G. Lowrie, and J. M. Lazarus, *New Engl. J. Med.* **329**, 1001 (1993).
3. T. F. Parker, L. Husni, W. Huang, N. Lew, and E. G. Lowrie, *Am. J. Kidney Dis.* **23**, 670 (1994).
4. 1999 Annual Report, End State Renal Disease Clinical Performance Measures Project. Department of Health and Human Services, Health Care Financing Administration, Office of Clinical Standards and Quality (Baltimore, Maryland, December 1999).
5. L. A. Szczech, E. G. Lowrie, Z. Li, N. L. Lew, J. M. Lazarus, and W. F. Owen, Jr., *Kidney Int.* **59**, 738 (2001).
6. E. Klein, J. G. Montalvo, R. Wawro, F. F. Holland, and A. Lebeouf, *Int. J. Artificial Organs* **1**, 16 (1978).
7. P. R. Keshaviah, J. P. Ebben, and P. F. Emerson, *Pediatric Nephrology* **9**, S2 (1995).
8. S. Zamponi, B. L. Cicero, M. Mascini, L. D. Ciana, and S. Sacco, *Talanta* **43**, 1373 (1996).
9. P. Jacobs, W. Sansen, and R. Homrouckx, *ASAIO J* **40**, M393 (1994).
10. C. V. Eddy and M. A. Arnold, *Clin. Chem.* **47**, 1279 (2001).
11. P. R. Jensen and J. Bak, *Appl. Spectrosc.* **56**, 1600 (2002).
12. T. T. Ngo, A. P. H. Phan, C. F. Yam, and H. M. Lenhoff, *Anal. Chem.* **54**, 46 (1982).
13. E. V. Thomas, *Anal. Chem.* **66**, 795A (1994).
14. R. Kramer, *Chemometric Techniques for Quantitative Analysis* (Marcel Dekker, Inc, New York, 1998).
15. G. W. Small, L. A. Marquardt, and M. A. Arnold, *Anal. Chem.* **65**, 3279 (1993).
16. M. R. Riley, M. Rhiel, X. Zhou, M. A. Arnold, and D. W. Muhammad, *Biotechnol. Bioeng.* **55**, 11 (1995).
17. K. H. Hazen, M. A. Arnold, and G. W. Small, *Appl. Spectrosc.* **52**, 1597 (1998).
18. M. A. Arnold, J. Burmeister, and G. Small, *Anal. Chem.* **70**, 1773 (1998).
19. J. G. Bayly, V. B. Kartha, and W. H. Stevens, *Infrared Phys.* **3**, 211 (1963).
20. R. M. Silverstein, G. C. Bassler, and T. C. Morrill, Eds., *Spectrometric Identification of Organic Compounds* (John Wiley and Sons, New York, 1991), 5th ed., p. 122.
21. P. R. Griffiths and J. A. de Haseth, *Fourier Transform Infrared Spectrometry* (John Wiley and Sons, New York, 1986).